

CARDIOVASCULAR

# Non-invasive measurement of cardiac output using an iterative, respiration-based method

M. Klein<sup>1,2</sup>, L. Minkovich<sup>3</sup>, M. Machina<sup>3</sup>, M. Selzner<sup>4</sup>, V. N. Spetzler<sup>4</sup>, J. M. Knaak<sup>4</sup>, D. Roy<sup>3</sup>, J. Duffin<sup>1,2\*</sup> and J. A. Fisher<sup>2,3</sup>

<sup>1</sup> Department of Physiology, University of Toronto, Toronto, Ontario, Canada

<sup>2</sup> Thornhill Research Inc., Toronto, Ontario, Canada

<sup>3</sup> Department of Anaesthesia and <sup>4</sup> Department of Surgery, University Health Network, Toronto, Ontario, Canada

\* Corresponding author. E-mail: j.duffin@utoronto.ca

## Editor's key points

- Current non-invasive monitors of cardiac output suffer from significant practical limitations.
- A novel respiratory-based method involving sequential gas delivery to control alveolar ventilation is described and compared with bolus pulmonary artery thermodilution.
- This novel method was validated in a porcine model of liver transplantation, and is therefore a promising approach for further evaluation.

**Background.** Current non-invasive respiratory-based methods of measuring cardiac output ( $\dot{Q}$ ) make doubtful assumptions and encounter significant technical difficulties. We present a new method using an iterative approach ( $\dot{Q}_{IT}$ ), which overcomes limitations of previous methods.

**Methods.** Sequential gas delivery (SGD) is used to control alveolar ventilation ( $\dot{V}_A$ ) and  $\text{CO}_2$  elimination ( $\dot{V}_{\text{CO}_2}$ ) during a continuous series of iterative tests. Each test consists of four breaths where inspired  $\text{CO}_2$  ( $P_{I\text{CO}_2}$ ) is controlled; raising end-tidal  $P_{\text{CO}_2}$  ( $P_{E'\text{CO}_2}$ ) by about 1.33 kPa (10 mm Hg) for the first breath, and then maintaining  $P_{E'\text{CO}_2}$  constant for the next three breaths. The  $P_{I\text{CO}_2}$  required to maintain  $P_{E'\text{CO}_2}$  constant is calculated using the differential Fick equation (DFE), where  $\dot{Q}$  is the only unknown and is arbitrarily assumed for the first iteration. Each subsequent iteration generates measures used for calculating  $\dot{Q}$  by the DFE, refining the assumption of  $\dot{Q}$  for the next test and converging it to the true  $\dot{Q}$  when  $P_{E'\text{CO}_2}$  remains constant during the four test breaths. We compared  $\dot{Q}_{IT}$  with  $\dot{Q}$  measured by bolus pulmonary artery thermodilution ( $\dot{Q}_{TD}$ ) in seven pigs undergoing liver transplantation.

**Results.**  $\dot{Q}_{IT}$  implementation and analysis was fully automated, and  $\dot{Q}_{TD}$  varied from 0.6 to 5.4 litre  $\text{min}^{-1}$  through the experiments. The bias (between  $\dot{Q}_{IT}$  and  $\dot{Q}_{TD}$ ) was 0.2 litre  $\text{min}^{-1}$  with 95% limit of agreement from  $-1.1$  to 0.7 litre  $\text{min}^{-1}$  and percentage of error of 32%. During acute changes of  $\dot{Q}$ , convergence of  $\dot{Q}_{IT}$  to actual  $\dot{Q}$  required only three subsequent iterations.

**Conclusions.**  $\dot{Q}_{IT}$  measurement is capable of providing an automated semi-continuous non-invasive measure of  $\dot{Q}$ .

**Keywords:** carbon dioxide; cardiac output; monitoring; respiration

Accepted for publication: 29 August 2014

Obtaining a measurement of cardiac output ( $\dot{Q}$ ) that is practical, accurate, non-invasive, continuous, and fully automated is highly desirable in clinical practice.<sup>1</sup> Indeed, monitoring  $\dot{Q}$  is a mandatory part of haemodynamic goal-directed therapy,<sup>2</sup> where prompt implementation can improve outcomes in high-risk patients.<sup>3,4</sup> Currently, the clinical standard for measuring  $\dot{Q}$  is bolus thermodilution ( $\dot{Q}_{TD}$ ). Unfortunately, the pulmonary artery catheter (PAC) required is invasive, with possibly life-threatening complications.<sup>5,6</sup>

The non-invasive Fick measurement of  $\dot{Q}$  (Fick  $\dot{Q}$ )<sup>7–10</sup> applies respiratory manoeuvres to determine  $\dot{Q}$ . However, despite its theoretical simplicity, Fick  $\dot{Q}$  has practical difficulties. All Fick  $\dot{Q}$  methods require two measures of steady-state arterial  $P_{\text{CO}_2}$  ( $P_{a\text{CO}_2}$ ) and  $\text{CO}_2$  elimination ( $\dot{V}_{\text{CO}_2}$ ) to calculate  $\dot{Q}$ : the first is

executed during a baseline period of stable ventilation and the second is executed after a perturbation in ventilation from the baseline state. In order to be valid, the second measurements must be obtained after the  $P_{a\text{CO}_2}$  and  $\dot{V}_{\text{CO}_2}$  have stabilized, but before the changes in  $P_{a\text{CO}_2}$  re-circulate to the lung. As the re-circulation time is short compared with the time it takes for  $P_{a\text{CO}_2}$  and  $\dot{V}_{\text{CO}_2}$  to stabilize, it is impossible to obtain a valid second measurement because during this short time, equilibrium between the pulmonary capillaries and alveoli does not occur.<sup>11</sup> In addition,  $P_{a\text{CO}_2}$  is estimated from end-tidal  $P_{\text{CO}_2}$  ( $P_{E'\text{CO}_2}$ ). While  $P_{E'\text{CO}_2}$  can provide a suitable estimate of  $P_{a\text{CO}_2}$  in healthy lungs, this approximation is not reliable where significant ventilation/perfusion ( $V/Q$ ) inequalities exist. Lastly, Fick  $\dot{Q}$  methods measure only the portion of  $\dot{Q}$  that perfuses

alveoli and participates in gas exchange. Blood flow through intrapulmonary shunts ( $\dot{Q}_s$ ) cannot be detected by Fick  $\dot{Q}$ .

We describe a novel method ( $\dot{Q}_{IT}$ ) that overcomes the re-circulation limitation of previous Fick  $\dot{Q}$  measures, using a series of short iterative tests. The reliability of  $\dot{Q}_{IT}$  is enhanced by pairing it with our previously developed technique of sequential gas delivery (SGD), allowing precise measures of  $\dot{V}_{CO_2}$  and more definitive estimates of  $P_{aCO_2}$  from  $P_{E'CO_2}$ . However, like previous Fick  $\dot{Q}$  methods,  $\dot{Q}_{IT}$  does not measure  $\dot{Q}_s$ . We present its theoretical derivation, a description of its implementation, and a proof-of-concept study comparing  $\dot{Q}_{IT}$  with  $\dot{Q}_{TD}$  in a porcine liver transplant model.

## Methods

### The Fick equations

Fick  $\dot{Q}$  is based on the mass balance principle: during any steady state, the  $O_2$  and  $CO_2$  exchange between pulmonary capillary blood and alveolar air is equal to the gas exchange between alveolar air and the environment.  $CO_2$  is used as a tracer because, unlike  $O_2$ , the relationship between  $CO_2$  tension and  $CO_2$  content in whole blood is virtually linear.<sup>12</sup>

As equation (1) shows,  $\dot{V}_{CO_2}$  can be expressed in terms of  $\dot{Q}$ , the difference between mixed venous and arterial  $CO_2$  tensions ( $P\bar{V}_{CO_2} - Pa_{CO_2}$ ) and the slope of the  $CO_2$  dissociation curve ( $S$ ).<sup>13</sup> Non-invasive end-tidal  $P_{CO_2}$  ( $P_{E'CO_2}$ ) usually substitutes for  $Pa_{CO_2}$ , ignoring any inequalities, which nevertheless can be quite significant [equation (2)].

$$\dot{V}_{CO_2} = \dot{Q} \times S \times (P\bar{V}_{CO_2} - Pa_{CO_2}) \quad (1)$$

$$\dot{V}_{CO_2} = \dot{Q} \times S \times (P\bar{V}_{CO_2} - P_{E'CO_2}) \quad (2)$$

For the differential Fick (DF) method,<sup>13</sup>  $\dot{V}_{CO_2}$  and  $P_{E'CO_2}$  are measured at baseline and during a reduction in alveolar ventilation ( $\dot{V}_A$ ). Assuming  $CO_2$  production remains constant during the test,  $\dot{V}_A$  reduction results in an increase in  $Pa_{CO_2}$  to a new steady state. The Fick mass balance equations for each of the baseline and test states are shown in equation (3a and b), where B and T superscripts refer to baseline and test states, respectively. Assuming  $P\bar{V}_{CO_2}$  is the same as baseline after the step reduction in  $\dot{V}_A$ , and assuming the test phase is completed *before re-circulation*, these two Fick equations are solved for  $\dot{Q}$ : the DF equation [equation (4)].

$$\dot{V}_{CO_2}^B = \dot{Q} \times S \times (P\bar{V}_{CO_2} - P_{E'CO_2}^B) \quad (3a)$$

$$\dot{V}_{CO_2}^T = \dot{Q} \times S \times (P\bar{V}_{CO_2} - P_{E'CO_2}^T) \quad (3b)$$

$$\dot{Q} = \frac{\dot{V}_{CO_2}^B - \dot{V}_{CO_2}^T}{S * (P_{E'CO_2}^T - P_{E'CO_2}^B)} \quad (4)$$

The DF avoids the difficulty of measuring  $P\bar{V}_{CO_2}$ , however DF has acknowledged limitations.<sup>11 14</sup> First, it erroneously assumes that any gradient between  $P_{E'CO_2}$  and  $Pa_{CO_2}$  remains constant and so affects both states equally. However, changes in alveolar gas concentrations during the test also change the gradients between  $Pa_{CO_2}$  and  $P_{E'CO_2}$ . Secondly, there is

insufficient time for  $P_{E'CO_2}^T$  to attain its new equilibrium before re-circulation, a limitation that applies to all Fick  $\dot{Q}$  techniques.<sup>11 15 16</sup> Finally, measuring  $\dot{V}_{CO_2}^T$  is technically challenging. We address all three issues by introducing SGD and an iterative approach.

### Sequential gas delivery

The core of the iterative method is the ability to precisely control  $\dot{V}_A$  by using an SGD breathing circuit.<sup>17 18</sup> In brief, the SGD circuit is configured with a non-rebreathing valve, an expiratory gas reservoir, and an inspiratory gas reservoir supplied by a flow-controlled gas blender. A one-way valve between the expiratory gas reservoir and the inspiratory limb enables re-breathing of previously expired gas *at the end of inspiration* to the extent that minute ventilation exceeds fresh gas flow to the circuit. Because exhaled gas has already equilibrated with pulmonary blood, it provides no gradient for gas exchange, and is 'neutral'. The blender gas flow is the only gas potentially available for gas exchange, regardless of minute ventilation, and therefore  $\dot{V}_A$  is equal to the blender gas flow, which is known *precisely* (to the accuracy of the gas blender). [When the  $P_{CO_2}$  of the inspired gas is  $>0$ , the flow of inspired gas can be conceptually divided into fresh gas and 'neutral' gas:  $\dot{V}_A = \text{total gas flow} (1 - P_{ICO_2}/Pa_{CO_2})$ .]<sup>17</sup> The partial pressure of  $CO_2$  in inspired gas ( $P_{ICO_2}$ ) is also known from the gas blender settings, and  $P_{E'CO_2}$  can be measured accurately by capnography;  $\dot{V}_{CO_2}^B$  and  $\dot{V}_{CO_2}^T$  are then known [equation (5a and b)].

$$\dot{V}_{CO_2}^B = \frac{\dot{V}_A \times (P_{E'CO_2}^B - P_{ICO_2}^B)}{PB} \quad (5a)$$

$$\dot{V}_{CO_2}^T = \frac{\dot{V}_A \times (P_{E'CO_2}^T - P_{ICO_2}^T)}{PB} \quad (5b)$$

Dividing by  $PB$  (barometric pressure corrected for the presence of water vapour) converts partial pressures into fractional concentrations.

The important advantage of SGD for measuring  $\dot{Q}$  is that first, it enables precise setting of alveolar ventilation (and thus  $\dot{V}_{CO_2}$ ) through control of fresh gas flow. Secondly, to the extent that rebreathed gas enters alveolar dead space, it brings gas concentrations closer to those of normally perfused alveoli and reduces ventilation-perfusion heterogeneity in the lung,<sup>19</sup> enabling end-tidal gas to better reflect alveolar gas,<sup>19</sup> and arterial blood gas.<sup>20-23</sup> As a result, sources of error for the parameters used to measure  $\dot{Q}$  ( $\dot{V}_{CO_2}^B$ ,  $\dot{V}_{CO_2}^T$ ,  $Pa_{CO_2}^B$ , and  $Pa_{CO_2}^T$ ) are reduced.

### Iterative approach

We use an iterative approach to address the inability to establish a new equilibrium  $Pa_{CO_2}$  after a step change in  $\dot{V}_{CO_2}^T$  before re-circulation. After establishing a baseline steady state,  $P_{E'CO_2}$  is raised by an arbitrary amount (about 1.33 kPa; 10 mm Hg) by delivering a bolus of  $CO_2$  during inspiration, and the resulting  $P_{E'CO_2}$  ( $P_{E'CO_2}^{T0}$ ) is noted. Thereafter, a  $P_{ICO_2}$  ( $P_{ICO_2}^T$ ) is calculated to maintain (clamp)  $P_{E'CO_2}$  at the level of  $P_{E'CO_2}^{T0}$  for the

subsequent three breaths of the test.  $P_{\text{ICO}_2}^{\text{T}}$  is calculated by substituting equation (5a and b) into equation (4) to obtain equation (6a), and re-arranging to solve for  $P_{\text{ICO}_2}^{\text{T}}$  [equation (6b)]. (Here,  $P_{\text{E}'\text{CO}_2}^{\text{T0}}$  replaces  $P_{\text{E}'\text{CO}_2}^{\text{T}}$  as it is this  $P_{\text{CO}_2}$  that we wish to clamp for the next three breaths.) Because  $\dot{Q}$  is unknown, an estimate ( $\dot{Q}^{\text{E}}$ ) is substituted, and  $P_{\text{ICO}_2}^{\text{T}}$  is computed. In the first iteration,  $\dot{Q}^{\text{E}}$  is guessed.

$$\dot{Q}^{\text{E}} = \frac{\dot{V}\text{A} \times (P_{\text{E}'\text{CO}_2}^{\text{B}} - P_{\text{ICO}_2}^{\text{B}}) - \dot{V}\text{A} \times (P_{\text{E}'\text{CO}_2}^{\text{T0}} - P_{\text{ICO}_2}^{\text{T}})}{S \times \text{PB} \times (P_{\text{E}'\text{CO}_2}^{\text{T0}} - P_{\text{E}'\text{CO}_2}^{\text{B}})} \quad (6a)$$

$$P_{\text{ICO}_2}^{\text{T}} = \frac{\dot{Q}^{\text{E}} \times S \times \text{PB} \times (P_{\text{E}'\text{CO}_2}^{\text{T0}} - P_{\text{E}'\text{CO}_2}^{\text{B}}) - \dot{V}\text{A} \times (P_{\text{ICO}_2}^{\text{B}} + P_{\text{E}'\text{CO}_2}^{\text{T0}} - P_{\text{E}'\text{CO}_2}^{\text{B}})}{\dot{V}\text{A}} \quad (6b)$$

Note that all parameters, other than  $\dot{Q}^{\text{E}}$ , on the right of equation (6b) are measured accurately or otherwise known. The  $P_{\text{E}'\text{CO}_2}$  from the last test breath ( $P_{\text{E}'\text{CO}_2}^{\text{T}}$ ) at this or any— $P_{\text{ICO}_2}^{\text{T}}$  is sufficient to calculate  $\dot{Q}$  using the DF [equation (7)].

$$\dot{Q} = \frac{\dot{V}\text{A} \times \{(P_{\text{E}'\text{CO}_2}^{\text{B}} - P_{\text{ICO}_2}^{\text{B}}) - (P_{\text{E}'\text{CO}_2}^{\text{T}} - P_{\text{ICO}_2}^{\text{T}})\}}{S \times \text{PB} \times (P_{\text{E}'\text{CO}_2}^{\text{T}} - P_{\text{E}'\text{CO}_2}^{\text{B}})} \quad (7)$$

Also note there is no tidal volume or respiratory rate in equation (6) or (7); they are subsumed by  $\dot{V}\text{A}$ , which is known precisely as it is equal to the blender gas flow to the SGD breathing circuit.

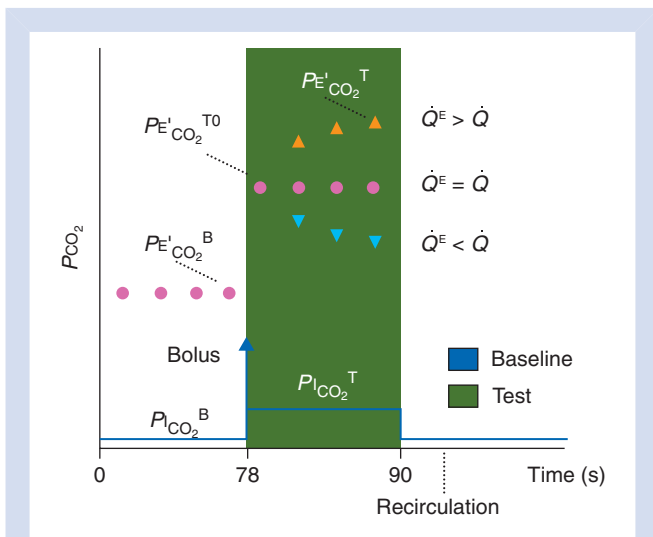


**Fig 1** Three possible results of the  $\dot{Q}_{\text{IT}}$  manoeuvre. An acute increase in inspiratory  $P_{\text{CO}_2}$  ('bolus') increases baseline  $P_{\text{E}'\text{CO}_2}^{\text{B}}$  to  $P_{\text{E}'\text{CO}_2}^{\text{T0}}$ . After the bolus, a  $\dot{Q}$  estimate  $\dot{Q}^{\text{E}}$  is used to compute the  $P_{\text{ICO}_2}$  necessary to maintain  $P_{\text{E}'\text{CO}_2}^{\text{T0}}$  constant for a short test period (shaded area). If the computed  $P_{\text{ICO}_2}$  produces a  $P_{\text{E}'\text{CO}_2}^{\text{T}}$  that maintains  $P_{\text{E}'\text{CO}_2}^{\text{T0}}$  constant during the test period, then  $\dot{Q}^{\text{E}}$  is equal to the actual  $\dot{Q}$ ; if not, then a drift upwards (triangles) or downwards (inverted triangles) in  $P_{\text{E}'\text{CO}_2}^{\text{T}}$  indicates over-estimation or under-estimation of  $\dot{Q}$ , respectively. In any case, sufficient data have been generated to calculate  $\dot{Q}$  by the DF equation [equation (7)].

If the arbitrarily chosen  $\dot{Q}^{\text{E}}$  happens to be correct, then the calculated  $P_{\text{ICO}_2}^{\text{T}}$  will be correct, and the  $P_{\text{E}'\text{CO}_2}^{\text{T0}}$  will remain constant during the delivery of  $P_{\text{ICO}_2}^{\text{T}}$ . But if  $\dot{Q}^{\text{E}}$  is not correct (most likely for the first guess),  $P_{\text{E}'\text{CO}_2}$  will exponentially approach an equilibrium value determined by  $P_{\text{ICO}_2}^{\text{T}}$  and the actual  $\dot{Q}$ . Figure 1 illustrates the three circumstances where the estimated  $\dot{Q}$  is too high, correct, or too low. Executing this test repeatedly, and using the DF equation (7) to calculate the next  $\dot{Q}^{\text{E}}$  to be used in equation (6b) converges  $\dot{Q}^{\text{E}}$  to the actual  $\dot{Q}$ .

## Animal experiments

The study was approved by the institution's animal care committee and conducted according to the guidelines of the Canadian Council on Animal Care. The  $\dot{Q}$  measurements were made in seven Yorkshire pigs weighing 27–34 (mean 30) kg that were undergoing orthotopic liver transplantation as part of an independent research project.<sup>24</sup> We reasoned that if the method functioned correctly under these widely variant, dynamic conditions, it should be sufficiently robust for most other clinical disorders.

Instead of the SGD circuit, described above in terms of valves and reservoir bags, we used a 'virtual' SGD compatible with an anaesthesia machine or ICU ventilator circuit. The specially designed proprietary software sensed inspiratory flows and injected  $\text{CO}_2$  in a pattern that simulated a physical SGD circuit, including the flow of fresh gas and the administration of neutral ('rebreathed') gas at end inspiration (see Supplementary Appendix SA for technical details).

## Animal preparation

Premedication consisted of i.m. administration of atropine (0.04 mg kg<sup>-1</sup>), ketamine (10 mg kg<sup>-1</sup>), and acepromazine (0.05 mg kg<sup>-1</sup>). Electrocardiogram, non-invasive arterial pressure (AP), heart rate, and pulse oximetry monitoring commenced using an AS/3 monitor (Datex-Ohmeda, Helsinki, Finland).

Anaesthesia induced with isoflurane (4–5%) using a large animal cone veterinary mask was maintained (after establishment of the airway) with isoflurane 1.5–2.5% (Vapor 19.1 Isoflurane vaporizer, Draeger, Telford, PA, USA). Lungs were ventilated with VT of 6 ml kg<sup>-1</sup>, RR of 20 bpm, I:E ratio=1:2, no PEEP, and  $F_{\text{I}\text{O}_2}=1$  (Narcomed 2C, Draeger). Dissection of the internal carotid artery (ICA) and internal jugular veins (IJVs) were performed via a median incision. The ICA was cannulated with a 20 G catheter (REF FA-04018, Arrow International, Reading, PA, USA). A 6 Fr introducer (Introflex™ CI500F6, Edwards Life Sciences, Irvine, CA, USA) was inserted into the IJV and paediatric PAC (135F5, Edwards Life Sciences) was advanced into the pulmonary artery.

Pressure transducers ( $P \times 3 \times 3272$ , Edwards Life Sciences) were zeroed at the level of mid-chest. AP, central venous pressure (CVP), and pulmonary artery pressure (PAP) were monitored and displayed continuously. Continuous observation of PAP and CVP waveforms confirmed correct position of the PAC. A Vigilance™ (Edwards Life Sciences) computer was used to measure  $\dot{Q}_{\text{TD}}$ .

The surgical techniques of OLT are described in detail elsewhere.<sup>25</sup> During the anhepatic phase, cross-clamping of the inferior vena cava (IVC), portal vein (PV), and hepatic artery was applied. A custom-made venous-venous bypass was used for venting the PV and IVC flows into the superior vena cava. The shunt consisted of an 8.5 Fr inflow cannula (Edwards Life Sciences) placed into the splenic vein and an 8.5 Fr outflow cannula inserted into the IJV contralateral to the PAC insertion. A 50 cm long tube connected the inflow and outflow cannulas. Blood was impelled through the bypass by the pressure gradient across the venous cross-clamps. Administration of fluids, vasoconstrictors, and inotropes was left to the discretion of the anaesthesia provider.

$\dot{Q}_{TD}$  was determined as the average of four sequential injections of 5 ml of iced (0–3°C) normal saline into the right atrium port of the PAC. Fluid infusions were stopped before  $\dot{Q}_{TD}$  measurements. Only measurements with a proper thermodilution curve and with a variation <20% between individual injections were included in the final analysis.  $\dot{Q}_{IT}$  measurements were commenced after initiation of mechanical ventilation and maintained thereafter every 90 s (~80 s baseline, 12 s test). The performance of the  $\dot{Q}_{IT}$  tests was fully automated requiring no operator input. Because of a large metabolic release of CO<sub>2</sub> after sodium bicarbonate administration,  $\dot{Q}_{IT}$  measurements obtained within the next 5 min were excluded. The  $\dot{Q}_{IT}$  measurement closest to the corresponding mean  $\dot{Q}_{TD}$  measurement was used for comparisons.

### Statistical analysis

Statistical analyses were accomplished using commercial software (SigmaPlot 12.5, Systat Software, Germany). Results are expressed as mean [standard deviation (SD)] unless otherwise specified. Pairs of  $\dot{Q}_{TD}$  and  $\dot{Q}_{IT}$  measurements were used to calculate a Pearson correlation coefficient, and the bias and limits of agreement by the method of Bland and Altman<sup>26</sup> modified for repeated measurements in the same subject.<sup>27–28</sup> Percentage error was calculated as 1.96 SD of the difference divided by the mean  $\dot{Q}$ .<sup>29</sup> Trending ability of  $\dot{Q}_{IT}$  to follow changes of  $\dot{Q}_{TD}$  was determined using the half-circle polar plot method, after applying an exclusion zone radius of 15% of the mean  $\dot{Q}$ .<sup>30</sup> An exponential function was fitted by the method of least squares to  $\dot{Q}_{IT}$  measurements obtained after acute changes of  $\dot{Q}$  (after IVC cross-clamping) to provide the time constant of convergence of  $\dot{Q}_{IT}$  to the true  $\dot{Q}$  value.

### Results

A total of 167 pairs of the mean  $\dot{Q}_{TD}$  and associated  $\dot{Q}_{IT}$  measurements were acquired during the OLT experiments. Figure 2 presents all  $\dot{Q}_{IT}$  and  $\dot{Q}_{TD}$  measurements. OLT was accompanied by profound changes of haemodynamic parameters, especially during the anhepatic and reperfusion stages (Fig. 3). The ranges of  $\dot{Q}_{TD}$  and  $\dot{Q}_{IT}$  measurements for all animals were 0.6–5.4 (mean 2.8) and 0.7–4.5 (mean 2.6) litre min<sup>-1</sup>, respectively. Despite multiple boluses of inspired CO<sub>2</sub> used by the  $\dot{Q}_{IT}$  method, the baseline (before each  $\dot{Q}_{IT}$  test)  $P_{E'CO_2}$  did not increase over time.

Linear regression analysis provided the equation  $\dot{Q}_{IT}=0.69\cdot\dot{Q}_{TD}+0.65$  with a Pearson correlation coefficient of 0.89. The Bland and Altman analysis showed a bias of -0.2 litre min<sup>-1</sup> with 95% limits of agreement from -1.1 to 0.7 litre min<sup>-1</sup> (Fig. 4). The percentage error between was 32%. The half-circle polar plot showed a mean radial bias of -7° with an SD and 95% confidence interval of the polar angle of 17° and 33°, respectively (Fig. 5).

The rate of convergence of the  $\dot{Q}_{IT}$  measurement after an acute change in  $\dot{Q}$  was computed after cross-clamping of the IVC and PV, accompanied by acute decrease in  $\dot{Q}_{IT}$  from 4.1 (0.8) to 1.7 (0.2) litre min<sup>-1</sup>. The time constant of convergence was 1.2 (0.2) iterations, so ~3 iterations (270 s) are required for 95% convergence. There was no relationship between the time constant of convergence and magnitude of change in  $\dot{Q}_{IT}$  ( $R^2=0.1$ ).

### Discussion

The main finding of this proof-of-concept study was that the novel respiratory iterative monitor  $\dot{Q}_{IT}$  is capable of providing a fully automated, semi-continuous, non-invasive measurement of  $\dot{Q}$ .  $\dot{Q}_{IT}$  implementation is feasible and easily adaptable to the respiratory circuits of an anaesthesia machine or an ICU ventilator. In the extreme OLT experiments in which profound shifts in  $\dot{Q}$  and other physiological parameters affect the accuracy of both  $\dot{Q}_{IT}$  and  $\dot{Q}_{TD}$  methods,  $\dot{Q}_{IT}$  displayed what would appear to be a clinically acceptable trending capability, albeit the percentage error (32%) barely exceeded the 30% limit, generally required to conclude that  $\dot{Q}_{TD}$  and  $\dot{Q}_{IT}$  might be used interchangeably in this experimental model. After acute changes of  $\dot{Q}$ ,  $\dot{Q}_{IT}$  converges to the actual  $\dot{Q}$  at a rate of about one time constant of equilibration per iteration, or 95% by the third iteration.

Contrary to prior Fick  $\dot{Q}$  methods,  $\dot{Q}_{IT}$  is based on reliable measures of all required parameters.  $P_{aCO_2}$  is derived from an accurate measure of  $P_{E'CO_2}$  equilibrated using SGD. SGD reduces ventilation-perfusion heterogeneity,<sup>20–22</sup> making  $P_{E'CO_2}$  equal to  $P_{aCO_2}$  within the error of measurement of each parameter in spontaneous breathing human subjects and in mechanically ventilated pigs with both normal and abnormal lungs.  $\dot{V}_{CO_2}$  is calculated from precisely known values of  $\dot{V}_A$ , which is equal to the fresh gas flow to the SGD circuit, and the  $P_{CO_2}$  of tidal gases. The previous limitation in obtaining an equilibration of respiratory gas with mixed venous gas before re-circulation occurs is addressed by an iterative approach that exponentially converges on the  $P_{VCO_2}-\dot{Q}$  pairs with each succeeding iterations. The smaller the drift of the  $P_{E'CO_2}$  values during the four breaths of the test, the closer is the  $\dot{Q}_{IT}$  calculation to actual  $\dot{Q}$ . When there is no drift, the  $\dot{Q}_{IT}$  calculation is theoretically equal to actual  $\dot{Q}$ .

Unlike other Fick  $\dot{Q}$ ,  $\dot{Q}_{IT}$  is able to assess the validity of the output of the algorithm. If  $\dot{Q}_{IT}$  and actual  $\dot{Q}$  converge,  $P_{E'CO_2}$  will be unchanged during the test phase, while  $\dot{Q}_E$  values above or below the actual  $\dot{Q}$  can be easily identified by an upward or downward drift in the  $P_{E'CO_2}$  tracing, respectively. Furthermore, the magnitude of drift indicates the magnitude of the discrepancy.

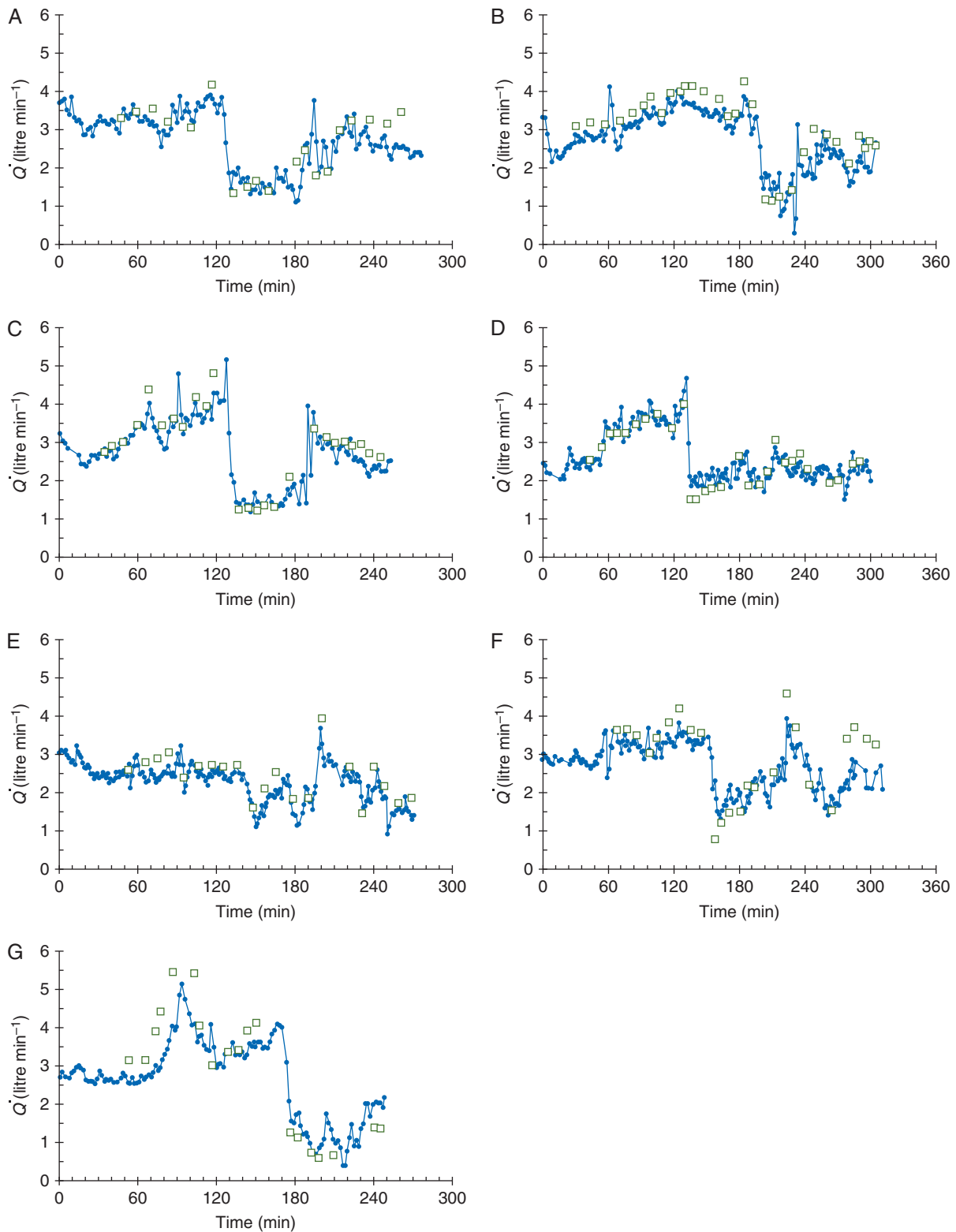


**Fig 2** (A–G) All  $\dot{Q}$  measurements in all seven experiments. Blue dots and lines are  $\dot{Q}_{IT}$  measurements and green squares are the mean of the last three of four  $\dot{Q}_{TD}$  measurements.

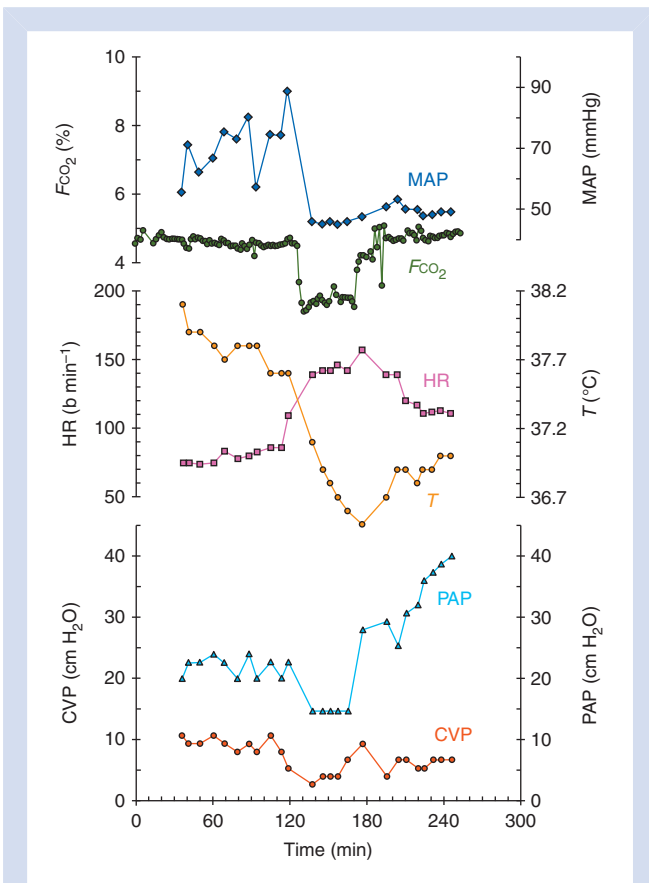


**Fig 3** A sample time series of cardiac output and other measurements during liver transplantation for Subject C, showing the corresponding baseline end-tidal fractions of  $F_{CO_2}$  (%); MAP, mean arterial pressure (kPa); HR, heart rate ( $\text{beats min}^{-1}$ );  $T$ , blood temperature ( $^{\circ}\text{C}$ ); CVP, central venous pressure (kPa); PAP, pulmonary artery pressure (kPa).

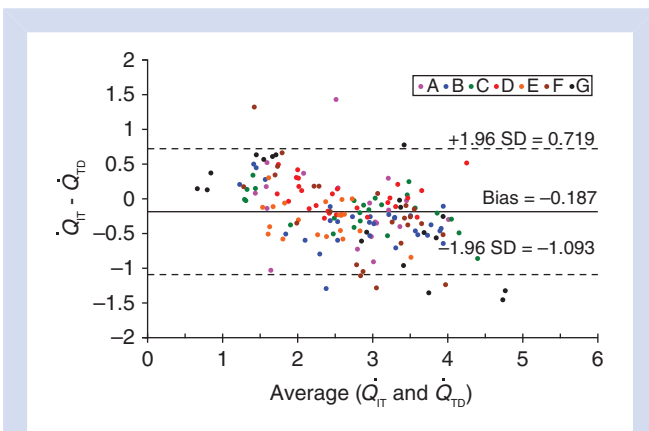


**Fig 4** A Bland-Altman analysis of the agreement of measurements.  $\dot{Q}_{IT}$ , iterative cardiac output;  $\dot{Q}_{TD}$ , bolus thermodilution cardiac output. Colour codes for experiments.

We suggest that the short time required for the  $\dot{Q}_{IT}$  test phase (12–15s) allows an increase in  $P_{E'CO_2}$  up to 1.33 kPa (10 mm Hg) with limited physiological impact of raising  $P_{aCO_2}$ .

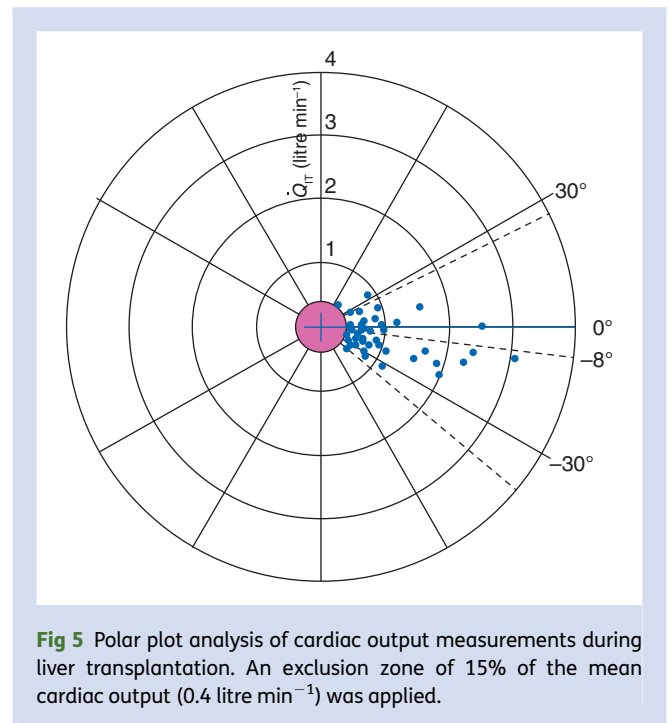


**Fig 5** Polar plot analysis of cardiac output measurements during liver transplantation. An exclusion zone of 15% of the mean cardiac output ( $0.4 \text{ litre min}^{-1}$ ) was applied.

(With 10 mm Hg increase in  $P_{E'CO_2}$ , as used in this study, an error of 1 mm Hg in the measure of  $P_{E'CO_2}$  at baseline or during the test phase would result in only 9–11% error in measured  $\dot{Q}_{IT}$ .) We found that baseline  $P_{E'CO_2}$  did not increase over time during these experiments. Nevertheless, the physiological effects of administering multiple  $CO_2$  boluses while performing  $\dot{Q}_{IT}$  must be addressed in further studies in models with normal and diseased lungs.

**Limitations**

We used  $\dot{Q}_{TD}$  as a reference technique because it is considered the clinical ‘gold standard’ for measurement of  $\dot{Q}$ . Consequently,  $\dot{Q}_{TD}$  will be the reference method against which  $\dot{Q}_{IT}$  will be validated in further clinical studies. However, we also appreciate that there are significant limitations in using  $\dot{Q}_{TD}$  as a reference in the OLT experiments. OLT was accompanied by abrupt and profound changes in blood temperature because of the large surgical exposure, incomplete mixing of unheated blood from the venous-venous bypass with venous return, and rapid infusions of i.v. fluids. These shifts of temperature affect measurements of  $\dot{Q}_{TD}$ .<sup>31</sup> We note that our experimental model did not include thoracotomy, and so we could not use an ultrasonic flow meter applied to the PA, which would be a better reference  $\dot{Q}$  technique.

As for all respiratory-based methods, the presence of severe lung disease can affect  $\dot{Q}_{IT}$  accuracy. Previous studies in dogs,<sup>32</sup> spontaneously breathing healthy humans,<sup>17 22</sup> and swine with lung disease<sup>20 21</sup> indicate that SGD markedly reduces the gradient between  $P_{E'CO_2}$  and  $P_{aCO_2}$  and so mitigates this source of error. However, the validity of  $\dot{Q}_{IT}$  for significant V/Q mismatch conditions should be confirmed in further studies.

To calculate  $\dot{Q}$ ,  $\dot{Q}_{IT}$  requires maintenance of a constant  $P_{E'CO_2}$  during the test period, which also serves as self-verification of accuracy. However, the degree of such constancy is not measured objectively and it remains a qualitative measure. We suggest that  $\dot{Q}_E$  has the greatest influence on the choice of the most effective  $P_{ICO_2}^T$ , but we did not measure the effect of imprecision for measures of  $P_{CO_2}$  and other non-systematic factors on the determination of  $\dot{Q}_{IT}$ .

Another limitation of any respiratory-based measurement of  $\dot{Q}$  is that blood flow that bypasses alveolar gas exchange is not measured. The validity of  $\dot{Q}_{IT}$  in the presence of high shunt fraction and high  $V_D/V_T$  should therefore be addressed in studies using appropriate experimental models. For example, our experimental model did not include animals with high  $\dot{Q}$ .

Lastly, this study was carried out in mechanically ventilated animals, and although  $\dot{Q}_{IT}$  is suitable for spontaneous ventilation (see Supplementary Appendix SB), it will need validation in further studies.

### Conclusions

We describe a novel fully automated respiratory-based method to measure cardiac output,  $\dot{Q}_{IT}$ , which overcomes a number of limitations of previous approaches. Our proof-of-concept study in the challenging model of OLT found acceptable bias and agreement between  $\dot{Q}_{IT}$  and the reference  $\dot{Q}_{TD}$ . While it provided a good estimation of cardiac output, it cannot be regarded as a reliable measurement until further evaluation experiments are performed.

### Supplementary material

Supplementary material is available at *British Journal of Anaesthesia* online.

### Authors' contributions

M.K. conceived the  $\dot{Q}_{IT}$  technique and designed, built and operated the system including the virtual SGD circuit software. All authors contributed to the drafting of the article. M.K., L.M., M.S., V.S., J.K., D.R., and J.F. contributed to the conception and design of the experiments. M.K., L.M., M.M., M.S., V.S., J.K., D.R., J.F., and J.D. contributed to the collection, analysis, and interpretation of the data, and M.K., J.D., L.M., and J.F. assisted in revising the manuscript critically for important intellectual content. The experiments were conducted at the Toronto General Hospital, University Health Network.

### Declaration of interest

J.F. is the chief scientist, J.D. is a senior scientist, and M.K. is an employee at Thornhill Research Inc. (TRI), a spin-off company from the University Health Network that developed the patented cardiac output measurement hardware and software.

### Funding

The study was supported by research grants of the Roche Organ Transplant Research Foundation (ROTRF), Astellas, and

Thornhill Research Inc. M.S. was supported by an ASTS Career Development Award. M.K. was supported by the Astellas Forschungsstipendium Transplantation 2011. We thank Uwe Mummehoff and the Birmingham family for their generous support.

### References

- 1 Marik PE. Noninvasive cardiac output monitors: a state-of-the-art review. *J Cardiothorac Vasc Anesth* 2013; **27**: 121–34
- 2 Aya HD, Cecconi M, Hamilton M, Rhodes A. Goal-directed therapy in cardiac surgery: a systematic review and meta-analysis. *Br J Anaesth* 2013; **110**: 510–7
- 3 Hamilton MA, Cecconi M, Rhodes A. A systematic review and meta-analysis on the use of preemptive hemodynamic intervention to improve postoperative outcomes in moderate and high-risk surgical patients. *Anesth Analg* 2011; **112**: 1392–402
- 4 Otero RM, Nguyen HB, Huang DT, et al. Early goal-directed therapy in severe sepsis and septic shock revisited: concepts, controversies, and contemporary findings. *Chest* 2006; **130**: 1579–95
- 5 Evans DC, Doraiswamy VA, Prosciak MP, et al. Complications associated with pulmonary artery catheters: a comprehensive clinical review. *Scand J Surg* 2009; **98**: 199–208
- 6 Reuter DA, Huang C, Edrich T, Shernan SK, Eltzschig HK. Cardiac output monitoring using indicator-dilution techniques: basics, limits, and perspectives. *Anesth Analg* 2010; **110**: 799–811
- 7 Jaffe MB. Partial CO<sub>2</sub> rebreathing cardiac output—operating principles of the NICO system. *J Clin Monit Comput* 1999; **15**: 387–401
- 8 Cade WT, Nabar SR, Keyser RE. Reproducibility of the exponential rise technique of CO<sub>2</sub> rebreathing for measuring P(v)CO<sub>2</sub> and C(v)CO<sub>2</sub> to non-invasively estimate cardiac output during incremental, maximal treadmill exercise. *Eur J Appl Physiol* 2004; **91**: 669–76
- 9 Peyton PJ, Thompson D, Junor P. Non-invasive automated measurement of cardiac output during stable cardiac surgery using a fully integrated differential CO<sub>2</sub> Fick method. *J Clin Monit Comput* 2008; **22**: 285–92
- 10 Hällsjö Sander C, Hallbäck M, Wallin M, Emtell P, Oldner A, Björne H. Novel continuous capnodynamic method for cardiac output assessment during mechanical ventilation. *Br J Anaesth* 2014; **112**: 824–31
- 11 Yem JS, Tang Y, Turner MJ, Baker AB. Sources of error in noninvasive pulmonary blood flow measurements by partial rebreathing: a computer model study. *Anesthesiology* 2003; **98**: 881–7
- 12 Loeppky JA, Luft UC, Fletcher ER. Quantitative description of whole blood CO<sub>2</sub> dissociation curve and Haldane effect. *Respir Physiol* 1983; **51**: 167–81
- 13 Gedeon A, Forslund L, Hedenstierna G, Romano E. A new method for noninvasive bedside determination of pulmonary blood flow. *Med Biol Eng Comput* 1980; **18**: 411–8
- 14 Yem JS, Turner MJ, Baker AB, Young IH, Crawford ABH. A tidally breathing model of ventilation, perfusion and volume in normal and diseased lungs. *Br J Anaesth* 2006; **97**: 718–31
- 15 Collier CR. Determination of mixed venous CO<sub>2</sub> tensions by rebreathing. *J Appl Physiol* 1956; **9**: 25–9
- 16 Defares JG. Determination of PvCO<sub>2</sub> from the exponential CO<sub>2</sub> rise during rebreathing. *J Appl Physiol* 1958; **13**: 159–64
- 17 Slessarev M, Han J, Mardimae A, et al. Prospective targeting and control of end-tidal CO<sub>2</sub> and O<sub>2</sub> concentrations. *J Physiol* 2007; **581**: 1207–19
- 18 Somogyi RB, Vesely AE, Preiss D, et al. Precise control of end-tidal carbon dioxide levels using sequential rebreathing circuits. *Anaesth Intensive Care* 2005; **33**: 726–32

- 19 Brogan TV, Robertson HT, Lamm WJ, Souders JE, Swenson ER. Carbon dioxide added late in inspiration reduces ventilation–perfusion heterogeneity without causing respiratory acidosis. *J Appl Physiol* 2004; **96**: 1894–8
- 20 Fierstra J, Machina M, Battisti-Charbonney A, Duffin J, Fisher JA, Minkovich L. End-inspiratory rebreathing reduces the end-tidal to arterial PCO<sub>2</sub> gradient in mechanically ventilated pigs. *Intensive Care Med* 2011; **37**: 1543–50
- 21 Fierstra J, Winter J, Machina M, et al. Non-invasive accurate measurement of arterial PCO<sub>2</sub> in a pediatric animal model. *J Clin Monit Comp* 2013; **27**: 147–55
- 22 Ito S, Mardimae A, Han J, et al. Non-invasive prospective targeting of arterial PCO<sub>2</sub> in subjects at rest. *J Physiol* 2008; **586**: 3675–82
- 23 Willie CK, Macleod DB, Shaw AD, et al. Regional brain blood flow in man during acute changes in arterial blood gases. *J Physiol* 2012; **590**: 3261–75
- 24 Knaak M, Spetzler V, Goldaracena N, et al. Subnormothermic ex vivo liver perfusion reduces endothelial cell and bile duct injury after DCD pig liver transplantation. *Liver Transplant* 2014; **20**: 1296–305
- 25 Esmailzadeh M, Nickkholgh A, Majlesara A, et al. Technical guidelines for porcine liver allo-transplantation: a review of literature. *Ann Transplant* 2012; **17**: 101–10
- 26 Bland JM, Altman DG. Statistical methods for assessing agreement between two methods of clinical measurement. *Lancet* 1986; **i**: 307–10
- 27 Myles PS, Cui J. Using the Bland–Altman method to measure agreement with repeated measures. *Br J Anaesth* 2007; **99**: 309–11
- 28 Hamilton C, Stamey JD. Using a prediction approach to assess agreement between two continuous measurements. *J Clin Monit Comput* 2009; **23**: 311–4
- 29 Critchley LA, Critchley JA. A meta-analysis of studies using bias and precision statistics to compare cardiac output measurement techniques. *J Clin Monit Comput* 1999; **15**: 85–91
- 30 Critchley LA, Yang XX, Lee A. Assessment of trending ability of cardiac output monitors by polar plot methodology. *J Cardiothorac Vasc Anesth* 2011; **25**: 536–46
- 31 Feltracco P, Biancofiore G, Ori C, Saner FH, Della Rocca G. Limits and pitfalls of haemodynamic monitoring systems in liver transplantation surgery. *Minerva Anestesiol* 2012; **78**: 1372–84
- 32 Swenson ER, Robertson HT, Hlastala MP. Effects of inspired carbon dioxide on ventilation–perfusion matching in normoxia, hypoxia, and hyperoxia. *Am J Respir Crit Care Med* 1994; **149**: 1563–9

Handling editor: H. C. Hemmings